Theoretical Chemistry Accounts (2019) 138:66
https://doi.org/10.1007/s00214-019-2453-y

REGULAR ARTICLE

Effect of the alkyl substituent in NONOates derivatives on the reaction mechanism of NO liberation

Violeta Rangel-Galván[1] · María Eugenia Castro[2] · Jose Manuel Perez-Aguilar[1] · Norma A. Caballero[3] · Francisco Javier Meléndez[1]

Received: 22 February 2019 / Accepted: 20 April 2019 / Published online: 7 May 2019

Abstract

Nitric oxide (NO) is a small biological molecule dealing with several physiological processes. NO can be obtained from different donor compounds. In this work, an analysis of the reaction mechanism for the liberation of NO from a series of NONOates: 1,1-dimethyl-3-oxotriazan-2-olate $(CH_3)_2N[N(O)NO]^-$ (**1**), 1,1-diethyl-3-oxotriazan-2-olate $(CH_2CH_3)_2N[N(O)NO]^-$ (**2**), 1,1-dipropyl-3-oxotriazan-2-olate $(CH_2CH_2CH_3)_2$ $N[N(O)NO]^-$ (**3**), 1,1-dibutyl-3-oxotriazan-2-olate $(CH_2CH_2CH_2CH_3)_2N[N(O)NO]^-$ (**4**) and 1,1-dipenthyl-3-oxotriazan-2-olate $(CH_2CH_2CH_2CH_2CH_3)_2N[N(O)NO]^-$ (**5**) is carried out. M06L/6-311++G(d,p) density functional theory calculations were performed for obtaining the geometries and energies of the involved species in the mechanism. Mechanism is proposed by protonation of **1**–**5**, and then, their protonated tautomers are involved to obtain the intermediaries and transitions states. Tautomerization energies are found to be between 2.23 and 21.44 kcal mol^{-1} with respect to the lowest energy tautomer **H1** in all NONOates structures. Finally, as products, the corresponding secondary amine and two molecules of NO are obtained. Geometry optimizations were carried out in aqueous solution using SMD. Current ΔG values take into account the thermochemical contributions of enthalpy and entropy at 298.15 K. The effect of substituent size on the dissociation energy barrier was analyzed finding similar values for dissociation of **1**–**5** NONOates. The NONOate **1** with smallest substituent has the lowest dissociation barrier of 4.78 kcal mol^{-1} and leads to most energetically stable products. As alkyl substituent is increased in size, the value of dissociation barrier is increased in 1.5–2.0 kcal mol^{-1} for 2–5 NONOates. Relative pk_a values and natural bond orbitals, NBO, are estimated using for the tautomers **H5** where the protonation site has the most acid behavior causing the NO generation.

Keywords NONOate derivatives · DFT methods · Tautomers · Energy profile · Dissociation energy · Relative pk_a

1 Introduction

Nitric oxide (NO) is a small biological molecule involved in a great number of physiological functions. NO carries out its biological functions through chemical reactions with a specific number of biomolecules; therefore, it is important to study in detail the molecular liberation mechanisms of NO

Published as part of the special collection of articles derived from the 11th Congress on Electronic Structure: Principles and Applications (ESPA-2018).

Electronic supplementary material The online version of this article (https://doi.org/10.1007/s00214-019-2453-y) contains supplementary material, which is available to authorized users.

✉ María Eugenia Castro
mareug.castro@correo.buap.mx

✉ Francisco Javier Meléndez
francisco.melendez@correo.buap.mx

[1] Lab. de Química Teórica, Centro de Investigación, Depto. de Fisicoquímica, Facultad de Ciencias Químicas, Benemérita Universidad Autónoma de Puebla, Edif. FCQ10, 22 Sur y San Claudio, Ciudad Universitaria, Col. San Manuel, C.P. 72570, Puebla, Puebla, Mexico

[2] Centro de Química, Instituto de Ciencias, Benemérita Universidad Autónoma de Puebla, Complejo de Ciencias, ICUAP, Edif. IC8, 22 Sur y San Claudio, Ciudad Universitaria, 72570 Puebla, Mexico

[3] Facultad de Ciencias Biológicas, Benemérita Universidad Autónoma de Puebla, Edif. BIO1, 22 Sur y San Claudio, Ciudad Universitaria, 72570 Puebla, Mexico

from donor compounds. In recent studies, it is shown that NO influences over wound repairing by regulating inflammation, cell proliferation, matrix deposition, angiogenesis, and remodeling processes [1]. It has also been studied that nitrite enzymatically reacts with deoxyhemoglobin to generate NO in the red blood cells, which acts as an endocrine carrier of NO in the circulation under low-oxygen condition. This process is involved in the inhibition of development of cancer [2]. Additionally, NO is part of the vascular inflammatory treating and heart failure [3], among other important physiological functions. In the brain, NO acts as interneuronal messenger and is involved in many neuronal functions related to disorders including epilepsy, schizophrenia, drug addiction, anxiety, major depression [4].

The amine-based *N*-diazeniumdiolates are extensively used as NO donors, and their biological and pharmaceutical roles have been widely studied as useful pharmaceutical tools due to their wide experimental half-lives [5]. These compounds have a general structure X-[N(O)NO], with amino moieties like X = RRN (called NONOates) being extensively studied because of their ability to release NO in neutral media at biological level [6]. Experimentally, it is known that diazeniumdiolate in basic solutions is neutralized or acidified for giving decomposition to the amine and NO. Experimentally, Keefer et al. [7] evaluated the substitution dependency on the decomposition of diazeniumdiolates. They determined possible intermediates along the path, suggesting the protonation on the amine nitrogen at physiological pH as the most probable mechanism for decomposition and measured pk_a values for dialkylamino diazeniumdiolates [7, 8]. However, the complete molecular mechanisms for NO liberation from NONOates donors are not fully known.

From theoretical point of view, ab initio methods [9] and density functional theory calculations have been used to explore the NONOates decomposition for NO liberation [10–12]. Hall et al. [9] proposed a reaction mechanism for NO liberation using HF/6-31G(d) and MP2/6-31G(d) theory levels, where the protonation sites were the oxygen atoms at $[N(O)NO]^-$ moiety of substituted diazeniumdiolates. However, in this proposal a second protonation on the amino nitrogen was necessary for NO release from protonated NO dimer. Later, Dutton et al. explored the mechanism for NO liberation from dialkylamino diazeniumdiolates using B3LYP/6-311+G(d) and CBS-QB3 theory levels. They obtained optimized geometries and thermodynamic properties (i.e., enthalpies and free energies for 298 K) using PCM model for aqueous solvation. Relative pK_a values were obtained for protonated species of diazeniumdiolates using their relation with ΔG_{aq} parameter. The measured pk_a of 4.5 for diethylamino diazeniumdiolate (DEA/NO) was used for the least acidic tautomer, and then, the other tautomers were relative to it. pK_a estimation and NBO analysis showed the oxygen in $[N(O)NO]^-$ moiety are the most basic sites on dimethylamino diazeniumdiolate, while the protonation on the amino nitrogen leads to spontaneous dissociation to the amine and the NO dimer [10]. In a subsequent work, isopropylamine diazeniumdiolate (IPA/NO) was studied for its pH-dependent decomposition. Authors predicted the production NO at lower pH upon protonation of the amine nitrogen from fragmentation of the amide/NO adduct using B3LYP/6-311+G(d) and CBS-QB3 theory levels with PCM and CPCM solvation models. This mechanism involved the HNO production from protonation of the terminal oxygen at the $[N(O)NO]^-$ group, the most basic site, and NO results from double protonation process [11]. Dealing with decomposition molecular mechanisms of NONOates, Shaikh et al. reported a study about spectroscopic, kinetic, and computational approaches of the NO liberation from amino diazeniumdiolates. A computed energy profile for the NO liberation from DEA/NO using B3LYP/6-31+G(d) theory level was presented in aqueous environment evaluated with COSMO model. Also, the mechanism was proposed as pH-dependent via tautomerization of protonated NONOates, with pk_a predicted to be 4.6 for DEA/NO and − 2.7 for protonated tautomer on amine nitrogen, obtaining the amine and NO as products. Authors reported kinetic parameters for decomposition of amino NONOates for supporting the proposed mechanism, concluding that the rate determining step involves the cleavage N–N single bond for liberation of NO dimer [12].

In the present work, the effect of the dialkyl substituent in NONOates on the reaction mechanism of NO liberation is evaluated by M06L/6-311++G(d,p) theory level. Complete energy profiles, NBO analysis, and predicted pk_a values are presented for giving insights of reactive sites involved in the NO liberation mechanism.

2 Methodology

2.1 Computational chemistry

Calculations were carried out by density functional theory with M06L functional [13] and 6-311++G(d,p) [14] basis set. All possible protonated tautomers were obtained for NONOates **1**–**5**, see Fig. 1. **H5** is directly involved in the reaction path. Geometry optimization of reactants, intermediaries, transition states, and products was obtained in aqueous solution using solvation model density (SMD) [15]. Harmonic vibrational frequency calculations were computed using the same level of theory for all the stationary points to ensure their assignation of local minima and transition states. Analysis of natural bond orbital, NBO [16], was carried out on the NONOates **1**–**5** and their protonated tautomers at the same theory level using SMD in aqueous solution. pk_a values were estimated using the Pliego and Riveros

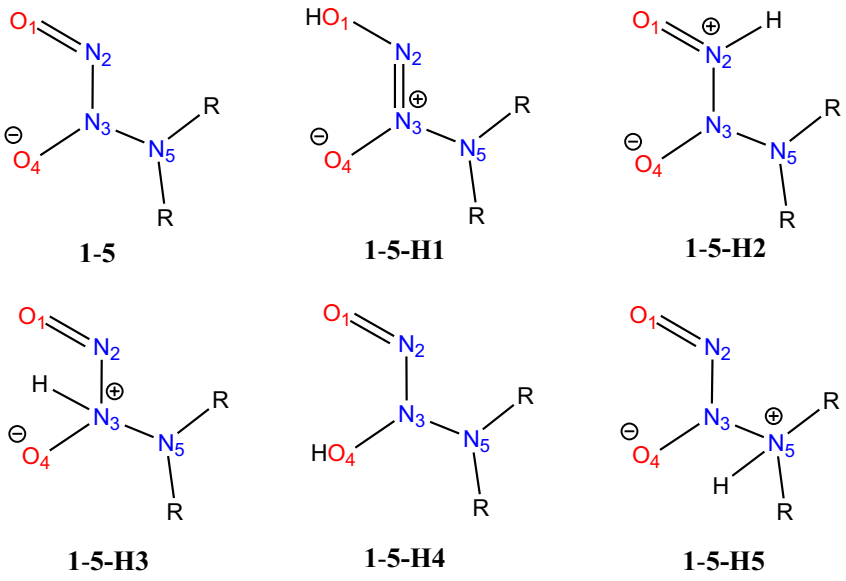

Fig. 1 Structures of NONOates **1**–**5** and their protonated tautomers **H1**–**H5**

R= -CH_3 (**1**); -CH_2CH_3 (**2**); -$(CH_2)_2$-CH_3 (**3**); -$(CH_2)_3$-CH_3 (**4**); -$(CH_2)_4$-CH_3 (**5**)

methodology [17] for the tautomers **1**–**5-H5**. All electronic structure calculations were performed using Gaussian16 program [18].

3 Results and discussion

3.1 Tautomers

Figure 2 presents the molecular structures for the optimized geometries of NONOates **1**–**5**. Non-protonated structures **1**–**5** are anionic structures with *Z* position for [N(O)NO]$^-$ moiety. The strong preference for the *Z* isomers of the dialkylamino diazeniumdiolate species has already been studied in previous theoretical studies [9–12]. Five tautomers were generated in the five possible protonation sites indicated in Fig. 1. Protonation on oxygen atoms in [N(O)NO]$^-$ moiety generates the tautomers **H1** and **H4**, while protonation on the nitrogen atoms produces the tautomers **H2** and **H3**. Protonation on the amino nitrogen generates the tautomer **H5**, which is used for NO liberation mechanism.

Table 1 summarizes the selected bond lengths for NONOates **1**–**5** and their protonated tautomers **H1-H5** in M06L/6-311++G(d,p) theory level in aqueous solvation with SMD. It can be observed the O1-N2 is increased from non-protonated NONOates to their corresponding tautomer **H1** while for **H2–H5** tautomers decreases. For N2–N3, a significant increase is observed for tautomer

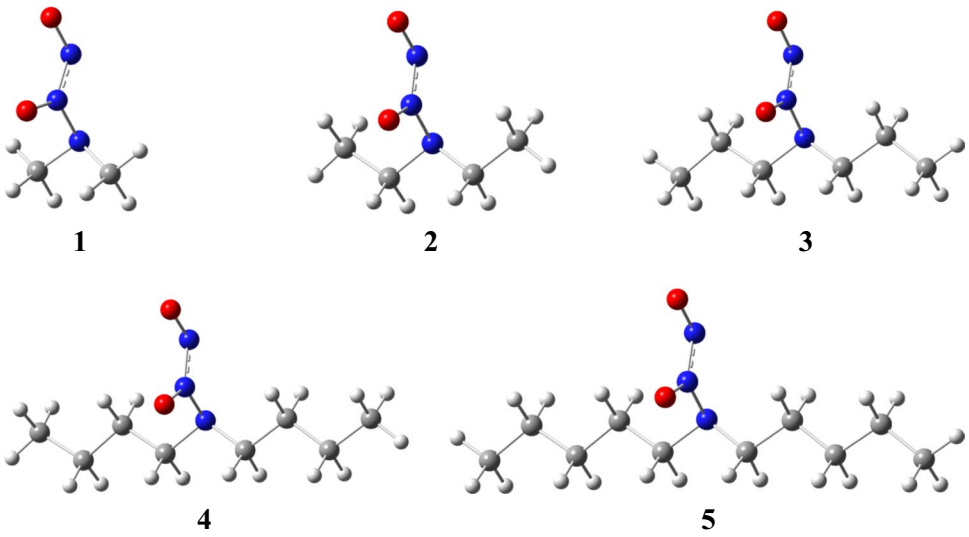

Fig. 2 Molecular structures for NONOates **1**–**5** calculated at M06L/6-311++G(d,p) level of theory with SMD in water

Table 1 Selected bond lengths (in Å) of NONOates **1–5** and their protonated tautomers **H1–H5** calculated at M06L/6-311++G(d,p) level of theory with SMD in water

	1	2	3	4	5
O1–N2					
Non-protonated	1.285	1.285	1.285	1.285	1.285
H1	1.368	1.355	1.355	1.355	1.355
H2	1.250	1.250	1.250	1.250	1.250
H3	1.139	1.141	1.141	1.141	1.241
H4	1.252	1.252	1.252	1.253	1.253
H5	1.267	1.266	1.266	1.266	1.266
N2–N3					
Non-protonated	1.305	1.306	1.306	1.306	1.306
H1	1.290	1.281	1.281	1.281	1.281
H2	1.305	1.306	1.306	1.306	1.306
H3	1.999	1.960	1.961	1.960	1.958
H4	1.301	1.302	1.302	1.302	1.302
H5	1.315	1.316	1.316	1.316	1.316
N3–O4					
Non-protonated	1.290	1.290	1.290	1.290	1.290
H1	1.260	1.259	1.259	1.259	1.259
H2	1.245	1.246	1.246	1.245	1.245
H3	1.269	1.284	1.284	1.284	1.284
H4	1.395	1.395	1.395	1.395	1.395
H5	1.259	1.261	1.261	1.261	1.261
N3–N5					
Non-protonated	1.290	1.431	1.432	1.433	1.432
H1	1.396	1.433	1.433	1.433	1.433
H2	1.436	1.432	1.434	1.434	1.434
H3	1.454	1.447	1.447	1.448	1.448
H4	1.368	1.365	1.366	1.366	1.366
H5	1.492	1.481	1.484	1.483	1.483

Numerical convention is used as Fig. 1

H3 (1.96–1.99 Å) while the rest of tautomers keep up a value about 1.28–1.31 Å close to that in non-protonated NONOates. Also, N3–O4 is only increased for tautomer **H4** (1.39 Å) from non-protonated NONOates, while the others maintain a value close to non-protonated NONOates (1.25–1.29 Å). For N3–N5, a slight increase is observed for protonated tautomers from non-protonated specie except for tautomer **H4**. In this case, it is relevant to underline that for non-protonated NONOate **1** and its tautomer **H1**, the distance N3–N5 is smaller than the rest of NONOates **2–5**. Bond length N3–N5 was previously reported as 1.491 Å at B3LYP/6-311+G(d) [10] for tautomer **1**-**H5** and 1.51 Å and B3LYP/6-31+G(d) [12] for **2-H5**, and both values are in agreement with our results. In general, according to Table 1, it can be observed that the values of bond lengths are kept up as the dialkylamino substituent is increased for NONOates **1–5**.

Table 2 Selected angles (in °) of NONOates **1–5** and their protonated tautomers **H1–H5** calculated at M06L/6-311++G(d,p) level of theory with SMD in water

	1	2	3	4	5
O1–N2–N3					
Non-protonated	113.72	113.60	113.67	113.64	113.66
H1	109.72	110.34	110.35	110.33	110.36
H2	122.93	123.00	122.99	123.00	123.00
H3	98.83	101.79	101.76	101.80	101.88
H4	113.26	113.22	113.22	113.20	113.21
H5	113.20	113.06	113.08	113.10	113.10
N2–N3–O4					
Non-protonated	126.29	126.01	126.09	126.08	126.08
H1	123.92	124.56	124.55	124.53	124.53
H2	122.41	122.28	122.32	122.34	122.33
H3	101.74	104.81	104.84	104.89	104.98
H4	119.97	119.77	119.77	119.75	119.76
H5	132.14	131.56	131.64	131.68	131.67
N5–N3–O4					
Non-protonated	120.35	120.33	120.33	120.28	120.32
H1	118.72	122.31	122.33	122.34	122.35
H2	124.83	124.92	124.92	124.92	124.92
H3	117.02	120.99	120.99	120.96	120.93
H4	118.39	118.39	118.41	118.41	118.42
H5	117.57	117.51	117.50	117.48	117.48
O1–N2–N3–O4					
Non-protonated	0.00	0.04	0.00	0.00	0.00
H1	2.83	0.08	0.00	0.00	0.01
H2	0.16	0.00	0.00	0.00	0.00
H3	1.11	5.22	−5.02	−4.69	4.63
H4	0.31	0.14	0.39	0.47	0.38
H5	−0.23	0.01	0.00	0.02	0.00
O1–N2–N3–N5					
Non-protonated	−179.99	179.83	179.99	179.98	−179.99
H1	−172.81	−179.73	179.98	179.99	−179.95
H2	−179.85	−179.99	179.99	179.98	−179.99
H3	−119.94	135.96	−135.73	−135.35	135.23
H4	179.54	179.60	178.71	178.45	178.71
H5	−179.66	−179.98	179.99	179.96	179.99

Numerical convention is used as Fig. 1

With respect to bond angles, in Table 2, the value of angle O1–N2–N3 was kept up for tautomers **H1**, **H4**, and **H5**, while for **H3** decreased in about 10°. Also, an increase about 10° was observed for **H2** in all NONOates. On the other hand, for N2–N3–O4 a decrease is observed for **H3**,

while an increase is found for **H5**. For N5–N3–O4, values are kept up around the value of 120° of non-protonated species. Similar values for angles O1–N2–N3, N2–N3–O4, and N5–N3–O4 were reported by tautomers of NONOate **1** and **2** in references [10, 12], respectively.

For dihedral angle O1–N2–N3–O4, it is observed that all tautomers for NONOates **1**–**5** prefer the *Z* conformation for $[N(O)NO]^-$ group. Only, slight deviations are observed for tautomer **H3**. For O1–N2–N3–N5, the tautomer **H3** suffers significant deviation for the conformation of dialkylamino substituent with respect to $[N(O)NO]^-$ group, while the rest of the tautomers maintain the atoms of the $[N(O)NO]^-$ group coplanar with amine nitrogen of the dialkylamino substituent (values in reality of 180°), see Table 2. Details of optimized structures are given in the SM in Table S1.

The optimized non-protonated NONOates in gas phase are predicted to be relative electronic energies $\Delta E_g = 68.0–71.0$ kcal mol^{-1} and relative free energies $\Delta G_g = 64.0–66.0$ kcal mol^{-1} higher than those calculated with SMD solvation in water (as present in Fig. 2). However, the tautomers **H1**–**H5** have only $\Delta E_g = 4.3–25.0$ kcal mol^{-1} and $\Delta G_g = 4.0–23.0$ kcal mol^{-1} with respect to optimized geometries in SMD. Relative free energies in gas phase and aqueous solvation free energies are shown in Table 3. Detailed values for energies are summarized in Table S2. In general, the tautomerization free energies are endergonic in water. Optimization in water predicts tautomer **H1** is the most energetically favorable, closely followed by tautomers **H4** and **H5** for the five NONOates. Considerable stabilization is observed when the aqueous solvent effect is taken into account including the thermochemical contributions of enthalpy and entropy at 298.15 K for change of standard state at 1 bar pressure and 1 M concentration. The relative free energies follow the trend **H1** < **H4** < **H2** < **H3** < **H5** in gas phase and **H1** < **H4** < **H5** < **H2** < **H3** in aqueous solution using SMD. This last trend is similar to that reported previously for dimethylamino diazeniumdiolate in Ref. [10] using CBS-QB3 with PCM model and for DEA/NO reported in Ref. [12] using B3LYP/6-31+G(d) with COSMO model for solvation. The great stabilization of **H5** tautomer in the five NONOates with SMD solvation could be attributed to the disposition for the spontaneous dissociation in gas phase observed in protonated amino diazeniumdiolates as it was obtained in previous study using B3LYP functional [10]. In our case, using M06L/6-311++G(d,p) theory level, although the fully optimization in gas phase does not lead to the dissociation of NO dimer, a lengthening of the bond distance N3–N5 (1.528, 1.534, 1.530, 1.554, and 1.517 Å) is observed with respect to their corresponding bond lengths in solution phase (1.492, 1.481, 1.484, 1.483, and 1.483 Å), see Table 3. Values of hydration free energies, calculated as $\Delta G_{hyd} = G_s - G_g$, where s indicates solution phase and g indicates gas phase, show higher negative values for non-protonated species, followed by tautomers **H5**. ΔG_{hyd} can be used as a measurement of the interaction between the solute with the solvent. In this case, negative values of ΔG_{hyd} correspond to a strong interaction between the compound with the water molecules for tautomer **H5**, which is proposed as the more labile reactant for liberation NO mechanism.

Table 3 Calculated ΔG (in kcal mol^{-1}) of NONOates **1**–**5** and their protonated tautomers **H1**–**H5** at M06L/6-311++G(d,p) level of theory in gas phase and SMD in water

NONOate	ΔG_{gas}	ΔG_{SMD}	ΔG_{hyd}
1	347.23	283.04	−64.19
1-H1	0.00	0.00	0.00
1-H2	15.97	10.81	−5.15
1-H3	20.22	19.37	−0.84
1-H4	4.89	3.54	−1.34
1-H5	27.00	9.45	−17.55
2	343.85	281.02	−62.82
2-H1	0.00	0.00	0.00
2-H2	13.33	8.37	−4.95
2-H3	22.63	20.35	−2.27
2-H4	2.27	2.23	−0.04
2-H5	25.26	5.56	−19.69
3	343.04	281.33	−61.70
3-H1	0.00	0.00	0.00
3-H2	13.15	8.71	−4.43
3-H3	21.90	20.73	−1.16
3-H4	2.08	2.47	0.39
3-H5	22.58	6.04	−16.53
4	342.67	281.41	−61.26
4-H1	0.00	0.00	0.00
4-H2	13.04	8.87	−4.17
4-H3	22.14	21.11	−1.02
4-H4	2.13	2.82	0.69
4-H5	21.83	6.22	−15.61
5	342.29	281.79	−60.50
5-H1	0.00	0.00	0.00
5-H2	12.92	8.97	−3.95
5-H3	21.98	21.44	−0.54
5-H4	2.14	2.57	0.42
5-H5	22.68	5.91	−16.77

3.2 Reaction mechanisms

Upon optimization in gas phase of minima structures of tautomers **H1**–**H5** of NONOates **1**–**5**, spontaneous dissociation does not occur; however, transition states (TS) and intermediary structures (Int) in the path are directly dissociated to the amine and the NO dimer. In order to obtain the ΔG_{SMD}, all necessary thermodynamic contributions were taken into

account to perform calculations in gas phase from fully optimized geometries at M06L/6-311++G(d,p) theory level with SMD in water as single-point calculations. The presence of single imaginary vibrational mode in each transition state structure was verified through frequency calculations at same level of theory with SMD. Table 4 collects the relative free energies for the species involved in the reaction mechanism of NO liberation from tautomers **H5** of each NONOate in aqueous solvation. Dissociation barriers for tautomers **H5** via **TS 1–5-H5** are found at 4.8–6.7 kcal mol^{-1}. A slight increase in the ΔG_{dis} for dissociation is observed when dialkylamino substituent is increased in size. The general behavior of energy profiles for decomposition of tautomers **1–5-H5** can be observed in Fig. 3. Tautomer **1-H5** was predicted to provide the smallest barrier to N3–N5 cleavage as reaction coordinate in the exothermic dissociation to the products, obtaining the most energetically stable products as **amine 1** and two NO molecules. For tautomers **1–4-H5**, when dialkylamino substituent is increased, the energy barrier is slightly affected. The energy barriers for decomposition of **TS 1–5-H5** of tautomers **H1–H4** differ by only 1.5 kcal mol^{-1}. These results indicate that tautomers **H1–H5** possess similar energetic profiles and would be expected to decompose at similar rates even though the alkyl substituent is increased. The transition states found for the decomposition of tautomer **H5** of DEA/NO has been reported as 17.8 kcal mol^{-1} in Ref. [12], which value is very higher compared to our value of 6.29 kcal mol^{-1}. However, the structure for **TS2–H5** is found to be similar geometry with a value for N3–N5 of 1.89 Å and ν(N3–N5 stretching) = 146i, cm^{-1} [12] in comparison with our value of N3–N5 = 1.882 Å and ν(N3–N5 stretching) = 286i, cm^{-1}. It can be attributed to the different methodologies used. Details of optimized structures and computed energies of species involved in decomposition mechanism are given in Tables S1 and S2. The values for dissociation barriers are consistent for all NONOates calculated. The energy profiles illustrating the decomposition of tautomers **1-H5** and **5-H5** for the formation of their corresponding secondary amines **1** and **5** and

Table 4 Free energy values, ΔG (in kcal mol^{-1}) of species involved in the reaction mechanism of liberation of NO from tautomers **1–5-H5** calculated at M06L/6-311++G(d,p) level of theory with SMD in water

NONOate	ΔG_{dis}	ΔG_{hyd}
1-H5	0.00	0.00
TS1-H5	4.78	17.66
Int1-H5	−4.01	26.77
Amine1 + 2NO	−6.33	28.47
2-H5	0.00	0.00
TS2-H5	6.29	18.28
Int2-H5	−0.90	26.63
Amine2 + 2NO	−3.29	27.38
3-H5	0.00	0.00
TS3-H5	6.20	18.12
Int3-H5	−1.18	26.36
Amine3 + 2NO	−3.45	27.11
4-H5	0.00	0.00
TS4-H5	6.31	18.88
Int4-H5	−1.23	26.24
Amine4 + 2NO	−3.19	27.31
5-H5	0.00	0.00
TS5-H5	6.72	19.31
Int5-H5	−0.94	26.54
Amine5 + 2NO	−3.35	27.43

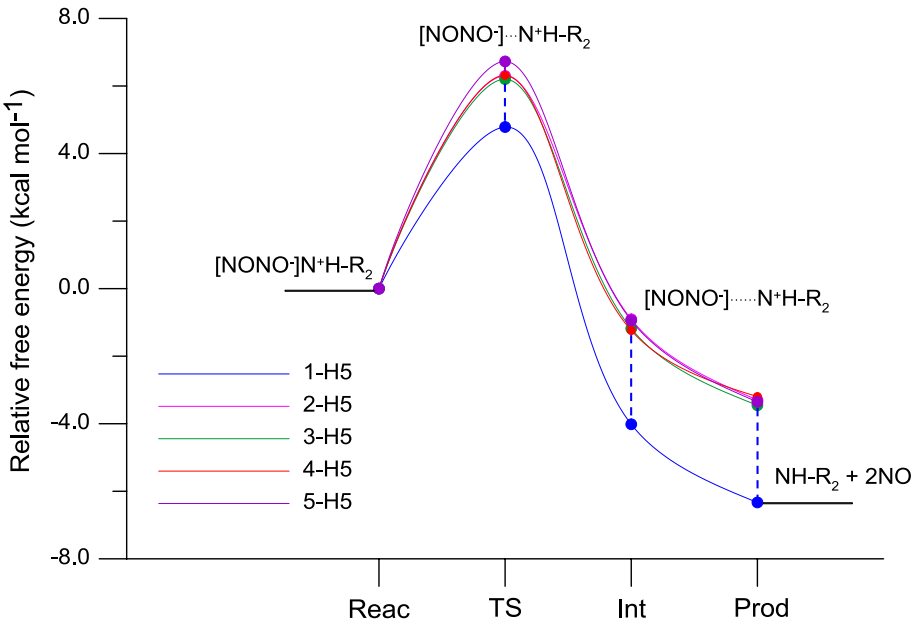

Fig. 3 General scheme of energy profiles for decomposition of tautomers **1–5-H5** for the liberation of NO calculated at M06L/6-311++G(d,p) level of theory. Reac refers reactant, TS is transition state, Int is intermediary, and Prod refers product

liberation of NO are shown in Fig. 4. The energy profiles for tautomers **2**–**4-H5** are illustrated in Fig. S1.

3.3 pK_a calculations and NBO analysis

As it has been mentioned, the tautomeric species **1**–**5**-**H5** are the direct participants in NONOates decomposition. Therefore, estimated pk_a values were calculated from tautomers **H5** and their corresponding non-protonated species **1**–**5**. The loss of proton from NONOates **1**–**5**-**H5** produces to five different non-protonated species according to the following Scheme 1.

Table 5 summarizes the values of relative free energies in gas phase and the solvation free energies for tautomers **1**–**5**-**H5** and their non-protonated species **1**–**5** using M06L/6-311++G(d,p) level of theory. The results show that tautomer **5-H5** with the largest substituent is more stable than tautomer **1-H5** at − 314.3 Hartrees. For non-protonated NONOates, **5** is 3.20 kcal mol^{-1} more stable than **1**.

The theoretical pk_a values were obtained with the objective to get insights about adequate physiological conditions to proton loss when the liberation of [N(O)NO]$^-$ groups is carried out. Estimated pk_a values were found based on the thermodynamic relations proposed by Pliego and Riveros

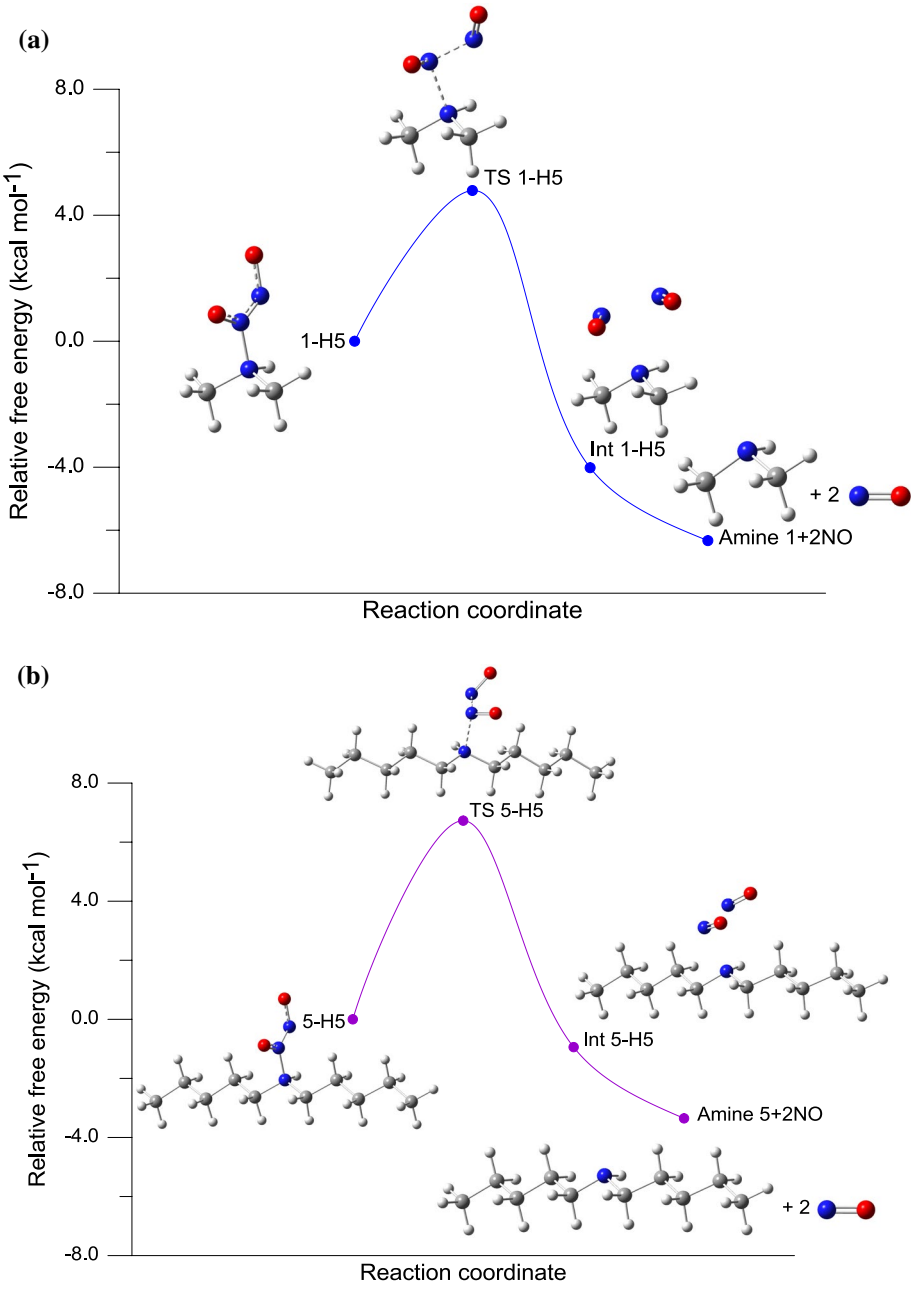

Fig. 4 Energy profile illustrating the decomposition of tautomer **a 1-H5** and **b 5-H5** for the formation the corresponding secondary amine and liberation of NO calculated at M06L/6-311++G(d,p) level of theory

Scheme 1 Formation of non-protonated species from NONOates **1**–**5**-**H5**

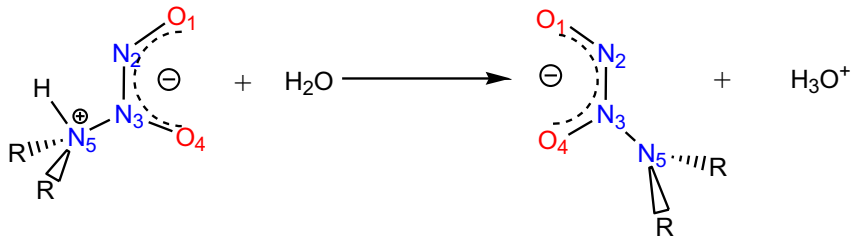

R= -CH_3 (**1**); -CH_2CH_3 (**2**); -$(CH_2)_2$-CH_3 (**3**); -$(CH_2)_3$-CH_3 (**4**); -$(CH_2)_4$-CH_3 (**5**)

Table 5 Relative free energy values in gas phase ($G°_g$) (in Hartrees) and solvation free energy values ($\Delta G°_s$) (in kcal mol^{-1}) for tautomers **1**–**5-H5** and non-protonated species **1**–**5** involved in the reaction mechanism of liberation of NO calculated at M06L/6-311++G(d,p) level of theory

NONOate	$G°_g$	$\Delta G°_s$	NONOate	$G°_g$	$\Delta G°_s$
1-H5	0.00	−32.08	1	0.00	−69.53
2-H5	−78.59	−31.97	2	−78.59	−68.73
3-H5	−157.18	−31.48	3	−157.18	−67.60
4-H5	−235.76	−31.00	4	−235.76	−67.02
5-H5	−314.34	−30.58	5	−314.34	−66.33

Table 6 Solvation free energy ($\Delta\Delta G°_s$) (in kcal mol^{-1}) and theoretical pk_a of tautomers **1**–**5-H5** involved in the reaction mechanism of NO liberation calculated at M06L/6-311++G(d,p) level of theory

NONOate	$\Delta\Delta G^0_S$ (kcal mol^{-1})	pK_a
1-H5 → 1	−177.65	−6.2
2-H5 → 2	−171.96	−1.8
3-H5 → 3	−168.32	0.5
4-H5 → 4	−164.22	3.4
5-H5 → 5	−160.65	5.6

[17] and following the acid–base theory according to Scheme 1. The equation used for estimating pk_a value is:

$$pK_a = \frac{\Delta G^0_{sol}}{1.364} - \log\left[H_2O\right]$$

where ΔG^0_{sol} is the difference of free energy between the species in aqueous solution, which is related to equation $\Delta\Delta G^0_{sol} = \Delta G^0_{solA^-} + \Delta G^0_{solH_3O^-} - \Delta G^0_{solHA} - \Delta G^0_{solH_2O}$. The solvation free energies of neutral species and their corresponding conjugated species as well as the water molecules were calculated using SMD model. For minimizing the calculation error in the computed pk_a, the experimental value of the free energy solvation for ion H_3O^+ of −110.2 kcal mol^{-1} was used, as it was suggested by Pliego and Riveros [17].

Table 6 shows the calculated pk_a of NONOates **1**–**5-H5**. Deprotonation of –NH group is associated with the pk_a values in ascending order. It means as the alkyl substituent is increased, a change in the pk_a value is observed from negative to positive values. Also, it is important to observe that deprotonation of N5 atom is favored in aqueous solution when the alkyl substituent is increased.

Previous theoretical pk_a estimations have been carried out using the relation $pk_a = -0.74(\Delta\Delta G_{aq}) + 4.5$ for *N*-protonated dimethylamino diazeniumdiolate with $pk_a = -8.9$ relative to 4.5 of the least acidic tautomer of DEA/NO. In this case, authors used the experimental pk_a of 4.5 of the DEA/NO, which is not that of the reactive site leading to decomposition. However, in their study these authors indicated that longer half-lives for NO production could arise by lowering pk_a of the amino nitrogen when the basic sites in the substituents are protonated [10]. Using the same approach, the pk_a value for DEA/NO was theoretically estimated as 4.6 and the *N*-protonated DEA/NO tautomer was estimated as −2.7 [12]. The pk_a predicted for IPA/NO was of 4.0 [11] using the method of Pliego and Riveros [13].

The natural bond orbital, NBO, analysis was realized on the tautomers **1**–**5-H5** for determining the electrostatic and bonding properties of these protonated species. Partial atomic charges of the atoms of $[N(O)NO]^-$ moiety from NBO analysis are summarized in Table 7. In general, similar values of atomic charges are obtained for the NONOates when the substituent is increased.

Partial atomic charges were previously reported [10] for $[N(O)NO]^-$ group using NBO analysis obtaining similar values (−0.60, 0.00, 0.26, −0.68, and −0.37) to the reported in Table 5 (−0.68, 0.02, 0.267, −0.681, and −0.36) for non-protonated NONOate **1**.

Figure 5 illustrates the NBO molecular graphs, as it can be observed no significant change is obtained with the increases in substituent. It means net charge is preserved in $[N(O)NO]^-$ group.

According to the charge distribution of the tautomers **1**–**5-H5** analyzed in Table 7 and Fig. 5, dipole moment (DM) was calculated to correlate the charge distribution in the non-protonated NONOates and protonated tautomers. Table 8 shows that DM values for tautomers **1**–**5-H5** are considerably larger than the other tautomers with values

Table 7 Natural bond orbitals (NBO) of NONOates **1**–**5** and their protonated tautomers **H1**–**H5** calculated at M06L/6-311++G(d,p) level of theory in SMD in water

	1	2	3	4	5
O1					
Non-protonated	−0.682	−0.679	−0.679	−0.679	−0.679
H1	−0.545	−0.519	−0.519	−0.519	−0.519
H2	−0.528	−0.524	−0.525	−0.525	−0.525
H3	−0.130	−0.140	−0.140	−0.140	−0.141
H4	−0.539	−0.537	−0.538	−0.538	−0.538
H5	−0.607	−0.602	−0.602	−0.602	−0.602
N2					
Non-protonated	0.027	0.030	0.030	0.030	0.030
H1	−0.003	0.066	0.066	0.066	0.066
H2	0.118	0.118	0.118	0.118	0.118
H3	0.274	0.282	0.282	0.282	0.282
H4	0.162	0.164	0.164	0.165	0.165
H5	0.040	0.039	0.039	0.039	0.039
N3					
Non-protonated	0.267	0.260	0.260	0.261	0.261
H1	0.372	0.345	0.346	0.346	0.346
H2	0.357	0.350	0.350	0.351	0.351
H3	0.036	0.028	0.030	0.030	0.031
H4	0.232	0.227	0.227	0.228	0.228
H5	0.270	0.263	0.263	0.264	0.264
O4					
Non-protonated	−0.681	−0.684	−0.683	−0.683	−0.683
H1	−0.556	−0.544	−0.543	−0.543	−0.543
H2	−0.508	−0.510	−0.509	−0.509	−0.509
H3	−0.599	−0.629	−0.628	−0.629	−0.629
H4	−0.551	−0.553	−0.553	−0.553	−0.553
H5	−0.581	−0.590	−0.588	−0.588	−0.588
N5					
Non-protonated	−0.362	−0.376	−0.371	−0.369	−0.369
H1	−0.278	−0.351	−0.346	−0.345	−0.344
H2	−0.352	−0.370	−0.365	−0.363	−0.363
H3	−0.371	−0.374	−0.369	−0.368	−0.368
H4	−0.308	−0.330	−0.320	−0.323	−0.322
H5	−0.265	−0.275	−0.271	−0.269	−0.269
C(−R)					
Non-protonated	−0.360	−0.166	−0.162	−0.160	−0.159
H1	−0.369	−0.169	−0.166	−0.163	−0.162
H2	−0.363	−0.167	−0.164	−0.161	−0.160
H3	−0.375	−0.177	−0.173	−0.170	−0.169
	−0.366	−0.169	−0.166	−0.163	−0.163
H4	−0.357	−0.161	−0.158	−0.155	−0.154
H5	−0.349	−0.152	−0.151	−0.147	−0.147

around 14.4 Debyes being similar to non-protonated species. It could indicate that charge and the substituent size play an important role in the DM value. DM is significantly increased when the size of dialkyl substituent increases of 11.1–14.7 Debyes in non-protonated species and 3.6–14.5 in the protonated tautomers. However, as it can be observed in Fig. 5 the charge distribution does not vary and, as a consequence, the DM direction either when substituent is increased.

Our calculations suggest a mechanism of decomposition via the direct protonation of the amine nitrogen as in early experimental [8] and theoretical [10–12] studies has suggested. Our calculations indicate slight variation in the dissociation barrier through the protonation of the amino nitrogen, tautomer **H5**, leading to decomposition for dialkylamino diazeniumdiolates when the dialkylamino substituent increases its size. Although NONOates can be protonated in five possible protonation sites, the NO liberation only occurs favorably and directly from tautomer **H5**. NONOates with substituents that contain terminal amines are currently being studied in more detail in order to study the effect of substituents with different chemical properties and size.

4 Conclusions

The theoretical studies for NO generation from diazeniumdiolate decomposition was performed using M06L/6-311++G(d,p) density functional theory calculations. The dialkylamino species were selected for increasing the substituent size, and all possible tautomers were generated by protonation. The relative stability of the tautomers varies in the gas phase and in aqueous solution.

The results suggest that the decomposition of dialkylamino diazeniumdiolates for NO generation with alkyl substituents increasing its size occurs via protonation on the amino nitrogen. It means the tautomers **H5**, assigned to the protonation on the amino nitrogen, provoke the exothermic dissociation of NONOates to corresponding secondary amine and NO dimer. The analysis of the mechanism of decomposition of NONOates to generate NO indicates that tautomer **H5** of NONOate **1** is slightly favored with the smallest free energy dissociation; however, no significant changes are found with the increase in the dialkylamino substituent chain. Previous studies were performed on dimethylamino diazeniumdiolate and diethylamino diazeniumdiolate (DEA/NO), which are in agreement with our structural and mechanistic results. The pk_a and NBO values provide insight into acid behavior and the atomic charge densities for tautomer **H5** of NONOates **1**–**5**.

In this context, it is important to know the mechanistic details by which dialkylamine NONOates are decomposed to produce NO, because it has demonstrated to be a signaling molecule of great importance for immunology, neurobiology, and cardiology. Improvements are necessary to

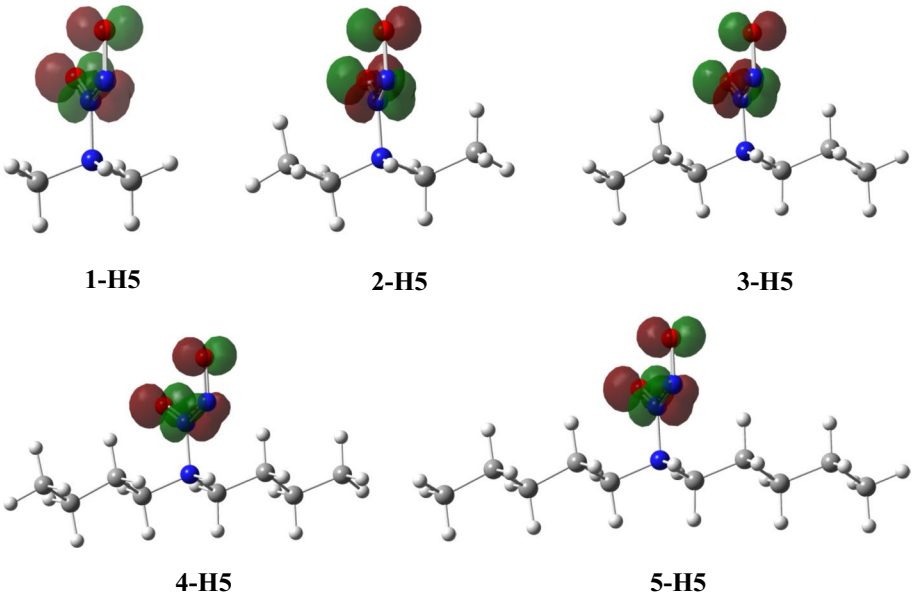

Fig. 5 NBO molecular graphs of tautomers **1**–**5**-**H5** calculated at M06L/6-311++G(d,p) level of theory in SMD in water

optimize the transition structures in gas phase which led to the products, suggesting these structures lay in shallow minima on the PES with small decomposition barriers. It should be attempted for dealing with other further strategies for calculation. The results obtained in this work should be of value for the design of other NONOates donors of NO. NONOates with zwitterionic structures with protonated terminal amines are currently being studied in more detail. We suggest further investigation about the intramolecular hydrogen bond of the different protonated tautomers as a stabilizing interaction in the aqueous solvation. Also, an important perspective of our research group is the study of different conformations of CNBD of HCN channel interacting with NO through dynamic molecular simulations for modeling the molecular mechanism close to the physiological medium conditions.

Table 8 Dipole moment DM (in Debyes) of NONOates **1**–**5** and their protonated tautomers **H1**–**H5** calculated at M06L/6-311++G(d,p) level of theory in SMD in water

NONOate	1	2	3	4	5
Non-protonated	11.141	12.119	13.421	13.931	14.652
H1	4.744	3.775	3.643	3.817	3.631
H2	7.981	8.081	8.014	8.110	8.005
H3	5.567	4.052	4.042	4.059	4.045
H4	5.716	5.781	5.647	5.825	5.636
H5	14.401	14.448	14.372	14.488	14.346

5 Supplementary material

Cartesian coordinates and energies of the different compounds optimized at the M06L/6-311++G(d,p) level of theory and energy profile for decomposition of tautomers H5.

Acknowledgements VRG thanks CONACYT-México for financial support (PhD fellowship No. 286497). Authors thank the Laboratorio Nacional de Supercómputo del Sureste de México (LNS-BUAP) of the CONACYT network of national laboratories, for the computer resources and support provided. Authors thank to VIEP-BUAP for the financial support, project: 100256733-VIEP2019, as well as the PRODEP Academic Group BUAP-CA-263 (SEP, Mexico).

References

1. Vimalraj S, Pichu S, Pankajam T, Dharanibalan K, Djonov V, Chatterjee S (2019) Nitric oxide regulates intussusceptive-like angiogenesis in wound repair in chicken embryo and transgenic zebrafish models. Nitric Oxide 82:48–58
2. Oronsky B, Oronsky N, Cabrales P (2018) Platelet inhibitory effects of the Phase 3 anticancer and normal tissue cytoprotective agent, RRx-001. J Cell Mol Med 22(10):5076–5082
3. Mughal A, Sun C, O'Rourke ST (2018) Activation of large conductance, calcium-activated potassium channels by nitric oxide mediates apelin-induced relaxation of isolated rat coronary arteries. J Pharmacol Exp Ther 366(2):265–273
4. Sanna MD, Monti M, Casella L, Roggeri R, Galeotti N, Morbidelli L (2015) Neuronal effects of a nickel-piperazine/NO donor complex in rodents. Pharmacol Res 99:162–173
5. Puglisi MP, Bradaric MJ, Pontikis J, Cabai J, Weyna T, Tednes P, Schretzman R, Rickert K, Cao Z, Andrei D (2018) Novel primary amine diazeniumdiolates—chemical and biological characterization. Drug Dev Res 79(3):136–143

6. Fitzhugh AL, Keefer LK (2000) Diazeniumdiolates: pro- and antioxidant applications of the "NONOates". Free Radic Biol Med 28(10):1463–1469
7. Habrie JA, Klose JR, Wink DA, Keefer LK (1993) New nitric oxide-releasing zwitterions derived from polyamines. J Org Chem 58:1472–1476
8. Davies KM, Wink DA, Saavedra JE, Keefer LK (2001) Chemistry of the diazeniumdiolates 2. Kinetics and mechanism of dissociation to nitric oxide in aqueous solution. J Am Chem Soc 123:5473–5481
9. Taylor DK, Bytheway I, Barton DHR, Bayse CA, Hall MB (1995) Toward the generation of NO in biological systems. Theoretical studies of the N_2O_2 grouping. J Org Chem 60:435–444
10. Dutton AS, Fukuto JM, Houk KN (2004) The mechanism of NO formation from the decomposition of dialkylamino diazeniumdiolates: density functional theory and CBS-QB3 predictions. Inorg Chem 43(3):1039–1045
11. Dutton AS, Suhrada CP, Miranda KM, Wink DA, Fukuto JM, Houk KN (2006) Mechanism of pH-dependent decomposition of monoalkylamine diazeniumdiolates to form HNO and NO, deduced from the model compound methylamine diazeniumdiolate, density functional theory, and CBS-QB3 calculations. Inorg Chem 45(6):2448–2456
12. Shaikh N, Valiev M, Lymar SV (2014) Decomposition of amino diazeniumdiolates (NONOates): molecular mechanisms. J Inorg Biochem 141:28–35
13. Zhao Y, Truhlar DG (2008) The M06 suite of density functionals for main group thermochemistry, thermochemical kinetics, noncovalent interactions, excited states, and transition elements: two new functionals and systematic testing of four M06-class functionals and 12 other functionals. Theor Chem Acc 120(1–3):215–241
14. Raghavachari K, Binkley JS, Seeger R, Pople JA (1980) Self-consistent molecular orbital methods. 20. Basis set for correlated wave-functions. J Chem Phys 72:650–654
15. Marenich AV, Cramer CJ, Truhlar DG (2009) Universal solvation model based on solute electron density and a continuum model of the solvent defined by the bulk dielectric constant and atomic surface tensions. J Phys Chem B 113:6378–6396
16. Reed AE, Curtiss LA, Weinhold F (1998) Intermolecular interactions from a natural bond orbital, donor-acceptor viewpoint. Chem Rev 88:899–926
17. Pliego JR Jr, Riveros JM (2002) Theoretical calculation of pK_a using the cluster-continuum model. J Phys Chem A 106:7434–7439
18. Frisch MJ, Trucks GW, Schlegel HB, Scuseria GE, Robb MA, Cheeseman JR, Scalmani G, Barone V, Petersson GA, Nakatsuji H, Li X, Caricato M, Marenich AV, Bloino J, Janesko BG, Gomperts R, Mennucci B, Hratchian HP, Ortiz JV, Izmaylov AF, Sonnenberg JL, Williams-Young D, Ding F, Lipparini F, Egidi F, Goings J, Peng B, Petrone A, Henderson T, Ranasinghe D, Zakrzewski VG, Gao J, Rega N, Zheng G, Liang W, Hada M, Ehara M, Toyota K, Fukuda R, Hasegawa J, Ishida M, Nakajima T, Honda Y, Kitao O, Nakai H, Vreven T, Throssell K, Montgomery JA Jr, Peralta JE, Ogliaro F, Bearpark MJ, Heyd JJ, Brothers EN, Kudin KN, Staroverov VN, Keith TA, Kobayashi R, Normand J, Raghavachari K, Rendell AP, Burant JC, Iyengar SS, Tomasi J, Cossi M, Millam JM, Klene M, Adamo C, Cammi R, Ochterski JW, Martin RL, Morokuma K, Farkas O, Foresman JB, Fox DJ (2016) Gaussian 16, Revision B.01. Gaussian, Inc., Wallingford